An improved multi-rule region growing method for point cloud segmentation of rock structural planes

Mengxi Sun¹, Yansong Duan¹, Hui Cao¹, Wei Qin¹

School of Remote Sensing and Information Engineering, Wuhan University, Wuhan 430079, China, mengxisun@whu.edu.cn, ysduan@whu.edu.cn, huicao@whu.edu.cn, wei-qin@whu.edu.cn

Keywords: Point Cloud Segmentation, Multi-rule Region Growing Proceedings, LiDAR, Structural Plane Extraction, Rock Structural Planes.

Abstract

Accurately and efficiently identifying rock mass structural planes and extracting their characteristic information is crucial for rock mass stability assessment. Three-dimensional (3D) laser scanning technology can significantly enhance both the efficiency and accuracy of structural plane surveying; however, current mainstream point cloud segmentation algorithms exhibit notable shortcomings, including blurred recognition of structural plane edges, insufficient segmentation accuracy, and poor integration precision among segmented blocks. To address these problems, this study proposes an improved multi-rule region growing point cloud segmentation method for rock structural planes. Specifically, plane fitting residuals are calculated from the point cloud data, and these residual values are then used to optimize seed point selection, thereby improving the segmentation accuracy of planar point sets. Next, considering the spatial relationship between the location of rock structural plane point clouds and their neighborhoods, a KD-tree data structure is employed to perform voxel downsampling for nearest-neighbor searching, and the RANSAC-based region growing algorithm is further refined. By adjusting the region growing segmentation parameters using multiple feature values and segmenting structural planes based on point cloud normal vector differences and final feature values, the proposed method facilitates the extraction of structural plane orientation, spacing, and extent, improving the overall segmentation quality. Experimental results demonstrate that the error between the segmented rock structural plane area and dimensions obtained by this method and those computed using CAD is only 1.07%, which meets the engineering error tolerance. Consequently, the proposed method provides stable and effective technical support for the identification and segmentation of rock structural planes.

1. Introduction

Rock mass stability assessment is of critical importance in geological engineering, mining, tunnel construction, and other related fields. As the weakest component within rock masses, rock structural planes—characterized by parameters such as orientation, trace length, strike, and dip-directly influence the mechanical behavior and stability of the rock mass. However, rock structural planes often exhibit interlaced distributions, and their complex geometric configurations and spatial relationships pose challenges to accurately and comprehensively identifying and evaluating them through traditional geological surveys. In recent years, the use of UAV photogrammetry and threedimensional laser scanning to acquire characteristic information of rock structural planes has enabled a more detailed representation of the three-dimensional features of rock masses, thereby providing more precise data for structural plane identification. Consequently, accurately recognizing and extracting characteristic information about rock structural planes has become a crucial task in rock mass stability evaluation.

In the process of extracting rock mass structural planes, especially under conditions where multiple planes are interlaced, existing point cloud segmentation methods face certain challenges. 3D point cloud region growing typically employs random sample consensus (RANSAC) to obtain seed points However, region growing based on RANSAC can be susceptible to segmentation instability, and when dealing with interwoven or complex geometries, it often suffers from insufficient segmentation accuracy. To overcome this limitation, Wang et al.

proposed a multi-scale supervoxel segmentation method for point cloud data by integrating multiple features such as color, reflectivity, normal vectors, and principal directions, followed by graph-based segmentation (Wang et al., 2021). However, this algorithm relies on analyzing various point cloud attributes, which constrains its range of application scenarios. Building on these approaches, Liu et al. constructed an undirected graph using voxels as nodes and employed connected components for clustering, followed by a refined segmentation of undersegmented objects via a normalized segmentation method (Haifeng et al., 2018). Nevertheless, this strategy requires filtering out ground points, which inevitably affects the segmentation of targets. Matsuzaki et al. randomly sampled seed points and determined whether their neighborhoods conformed to a pre-defined geometric model (Matsuzaki and Nonaka, 2024). However, this approach often suffers from false segmentations. Overall, while these methods have achieved notable progress, noise interference and blurred boundaries remain pressing handling complex structural challenges when Consequently, there is a strong need for further algorithmic optimization to enhance segmentation accuracy and efficiency.

In recent years, researchers have focused on automated or semiautomated extraction of structural plane parameters—such as orientation, spacing, and trace length—from three-dimensional (3D) point clouds of rock masses (Song et al., 2024). Traditional manual methods involve selecting at least three points on the structural plane to compute its normal vector, thereby obtaining the relevant parameters. This approach, however, is timeconsuming, prone to subjectivity, and yields incomplete geometric information. Another strategy involves either identifying principal curvature variations at point cloud vertices or searching for an optimal plane within the 3D model (Dumic and da Silva Cruz, 2025). Gigli et al. proposed a method wherein a cubic region is employed to search for coplanar point subsets, and clusters identified as belonging to the same structural plane are then merged (Gigli and Casagli, 2011). Nonetheless, the accuracy of this method is highly sensitive to the size of the cubic search region, leading to potential errors in cluster merging. Liu et al. presented a new structural plane grouping method that simultaneously considers orientation, trace length, and undulation (Liu et al., 2022). Nonetheless, the algorithm faces limitations in building high-density 3D point cloud models and accurately identifying and fitting complex structural planes, while also insufficiently addressing uncertainties in the statistical behavior of structural plane orientations. Meanwhile, Cao et al. developed a multi-task learning neural network that segments rock masses and calculates key parameters, facilitating accurate predictions of digital rock image segmentation, porosity, shear modulus, and bulk modulus (Cao et al., 2022). However, the relatively weak generalization capability of this model constrains its accuracy and robustness.

In response to the aforementioned issues, this paper proposes a multi-rule region growing method for rock structural plane segmentation in point clouds. Building upon the original RANSAC algorithm, novel sampling strategies and scoring criteria are introduced to improve region growing, while incorporating the specific attributes of structural planes to enhance segmentation accuracy and robustness in scenarios with complex interwoven structural planes. The main contributions of this study are as follows:

- 1. Proposing an improved RANSAC algorithm for finegrained segmentation of rock structural planes.
- 2. Proposing an improved Graham Scan algorithm for precise extraction of structural plane boundaries.
- 3. Employing nearest-neighbor searching to integrate larger structural plane clusters with adjacent smaller clusters, thereby enabling the extraction of critical structural plane information.

By leveraging the distinctive features of rock structural planes, the proposed method achieves efficient and noise-resilient structural plane recognition and segmentation, with the aim of providing a technical reference for the acquisition of foundational data on rock structural planes.

2. Method

To accurately segment structural surfaces and extract key geometric information from rock mass point clouds, this paper proposes an improved multi-rule region-growing method for rock mass structural surface point cloud segmentation. First, the seed point selection in the region-growing algorithm is optimized by calculating the local plane fitting residuals of the point cloud, which reduces initial segmentation errors. Next, by combining KD-tree voxel downsampling with the improved RANSAC strategy, the method ensures efficient processing of large-scale point cloud datasets while enhancing the reliability of plane fitting in noisy data environments. This effectively improves the algorithm's adaptability to complex and irregular rock structures. Finally, a multi-feature constraint method is introduced to refine the segmentation results based on point cloud normal vector differences and feature thresholds, enabling the extraction of key geometric information such as structural surface attitude, area, and dimensions. This provides valuable insights for geological

modeling and analysis. The specific implementation process of this method is illustrated in Figure 1.

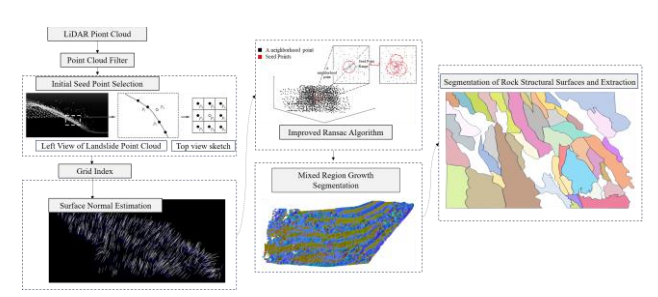


Figure 1. The general implementation flow of the method in this paper.

2.1 Improved Region Growing Algorithm

Region growing is a method of region segmentation based on the characteristics of the data. It compares the features of an arbitrary point with its surrounding points, merging data points with similar properties to achieve region identification and segmentation. The improved RANSAC algorithm proposed in this paper adopts a local sampling approach, obtaining new candidate planes in each iteration. At the same time, it calculates the score plane probability by considering both the number of points and the number of candidate planes, thus improving the plane fitting accuracy. Key issues that need to be addressed include: the selection of seed points, boundary judgment criteria, and the stopping condition for computation.

2.1.1 Seed Point Selection: This paper introduces multiple feature values to determine a characteristic terminal value, which replaces the traditional curvature scalar for point cloud sorting(Xu et al., 2023). The characteristic terminal value F is influenced by the spatial position of the points, with smaller F values indicating smoother regions. By selecting the point with the smallest characteristic terminal value as the initial point, the method ensures the rationality of the points while minimizing human interference, thus optimizing the computational results, as shown in Equation 1 and 2.

$$\begin{cases} O = (\lambda_1 \cdot \lambda_2 \cdot \lambda_3)^{\frac{1}{3}} \\ E = -\sum_{i=1}^{S} \lambda_i \cdot \ln \lambda_i \\ S = \lambda_3 / (\lambda_1 + \lambda_2 + \lambda_3) \\ V = 1 - |\langle [0 \quad 0 \quad 1], \vec{e}_3 \rangle| \end{cases}$$
(1)

$$F = \sqrt{O^2 + E^2 + S^2 + V^2} \tag{2}$$

Where λ_1 , λ_2 , and λ_3 represent the eigenvalues corresponding to the neighborhood point matrix, while O, E, S, and V denote the invariance of the point cloud, feature entropy, surface variation, and verticality, respectively. \vec{e}_3 represents the third eigenvector corresponding to the neighborhood point matrix.

2.1.2 Boundary Judgment Criteria: In natural environments, rock mass structural planes are typically formed by relatively regular planes and sharp edges. In field surveys, sharp edges are mainly used as boundaries, and structural planes with different orientations are grouped based on their characteristics. For the rock mass structural plane point cloud, planes with the same orientation should have the same or similar normal vectors. Therefore, the improved Graham Scan algorithm can be used to accurately segment the structural plane boundaries. The Figure 2 shows the boundary delineation results of the Graham Scan algorithm and the improved Graham Scan algorithm, respectively.

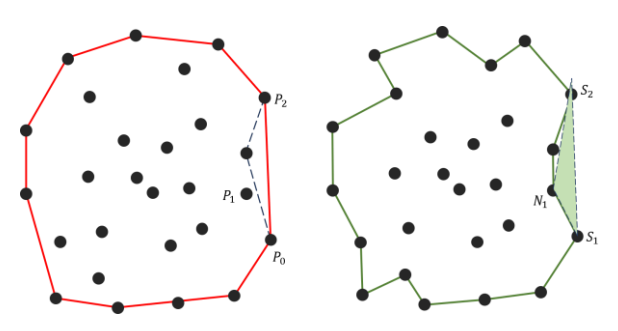


Figure 2. (a) Boundary detection using Graham Scan. (b) Boundary detection using modified Graham Scan.

For boundary points S_i and non-boundary points N_j , suppose there are two new lines, $S_1 N_1$ and $N_1 S_2$. If the triangle formed by these two new lines and $S_1 S_2$ does not contain any new boundary points, and the angle formed by $S_1 N_1$ and $N_1 S_2$ satisfies the tolerance for concave angles, N_1 will be considered a new boundary point. Additionally, the new boundaries can be determined using a recursive algorithm to calculate the new boundary points.

2.1.3 Cessation of Growth Conditions: Due to the large number of planes resulting from the exhaustive combinations of points in the computation, unlimited iterations of the data would waste significant resources and time. To ensure efficiency and accuracy, this paper introduces voxel downsampling with KD-tree nearest neighbor search, which controls the number of neighboring points while maintaining the original data's characteristics. Additionally, a maximum plane count T_{max} and confidence threshold are set to halt the normal vector calculation, while a minimum cluster size C_{min} is defined to stop the region growing process. During the computation, if Tmax is reached or if the result achieves sufficient confidence, the normal vector calculation can be stopped. Growth is halted when the number of points available for growth falls below C_{min} .

2.2 Structural Surface Information Extraction

2.2.1 Calculation of planar structure: The orientation of the structural plane is related to its azimuth. For point clouds, the corresponding attitude information must be derived through the normal vector. The attitude of the structural plane can be computed using the normal vector of the fitted plane, as described in Equation (3). Here, α represents the dip direction of the structural plane, and β represents the dip angle. In practical operations, the independent coordinate axes X and Y of the point cloud must correspond to the true east and true north directions, respectively.

$$\begin{cases}
\beta = \arccos c \\
s = \alpha/\sin \beta \\
\alpha = \arcsin s \quad a, b \ge 0 \\
\alpha = 360^{\circ} - \arcsin(-s) \quad a < 0, b > 0 \\
\alpha = 180^{\circ} - \arcsin s \quad a, b > 0 \\
\alpha = 180^{\circ} + \arcsin s \quad a > 0, b < 0
\end{cases}$$
(3)

The spacing between structural planes is typically characterized by the distance between structural planes within the same group. However, due to the inherent randomness of point cloud data, there are three primary factors that influence the calculation of spacing:

- 1. Variation in the size of structural planes: Structural planes vary in size, with larger clusters of structural planes adjacent to smaller clusters. This imbalance in the size distribution necessitates consideration of the differences in clustering when calculating the spacing between planes.
- 2. Irregularity of structural planes: Structural planes are often irregular, meaning they are not perfectly parallel to one another. The arrangement and angles between these planes may vary, requiring the calculation of spacing to account for the angular differences and their impact on the overall spacing.
- 3. Continuous and discontinuous states of structural planes: During the calculation, structural planes may exist in continuous or discontinuous states. In the continuous state, multiple structural planes are treated as a single unit, while in the discontinuous state, each plane is considered an individual unit.

Considering the aforementioned factors, this study integrates and sorts the larger clusters of structural planes and their adjacent smaller clusters using nearest-neighbor search. A two-dimensional projection plane is established to obtain the projection lines of the structural planes. Along the projection lines, orthogonal survey lines are constructed at fixed intervals. Finally, the distances between the intersection points of the orthogonal survey lines and the various projection lines are calculated, and the average of these distances is taken as the spacing between structural planes, as described in Equation (4).

$$\overline{G_{l,j}} = \frac{\sum_{i,j=1}^{n} \sqrt{\left[(x_i - x_j)^2 + (y_i - y_j)^2 \right]}}{n}$$
 (4)

In the equation, $\overline{G_{i,j}}$ represents the average distance between the projection lines of the structural planes (in meters), x_i and x_j denote the x-coordinate values of the two intersection points between the orthogonal survey lines and the projection lines, while y_i and y_j represent the y-coordinate values of the same intersection points. n is the predefined interval between the orthogonal survey lines.

In this paper, the extent of the structural plane is characterized by the length of the exposed discontinuous surface in the dip direction and strike direction. A transformation matrix is used to assign an independent coordinate system to the merged structural planes, and the length in the corresponding direction is calculated to determine the extent. The specific calculation is as shown in Equation (5) and (6):

$$\begin{cases} W = \cos \eta, X = \cos \theta \\ Y = \sin \eta, Z = \sin \theta \\ R = \begin{bmatrix} WZ - X & YZ \\ WX & Z & YX \\ -Y & 0 & W \end{bmatrix} \end{cases}$$
 (5)

$$LP_{\text{Dipdirection}} = \max(x') - \min(x')$$

$$LP_{\text{Direction}} = \max(y') - \min(y')$$
(6)

Here, θ and η represent the dip direction and dip angle of the merged structural plane, respectively. $LP_{\text{Dipdirection}}$ refers to the extent of the dip direction in meters, while $LP_{\text{Direction}}$ refers to the extent of the strike direction in meters. $\max(x')$ and $\min(x')$ represent the maximum and minimum values of the dip direction in the independent coordinate system, respectively, while $\max(y')$ and $\min(y')$ represent the maximum and minimum values of the strike direction in the independent coordinate system, respectively.

2.2.2 Calculation of Structural Surface Dimensions: The size of the structural surface reflects its dimensions. Based on the contour points identified by the improved Graham Scan algorithm in Section 2.1.2, the Ear Clipping algorithm is used for triangulation, as shown in Figure 3. When point A is at a convex angle, line segment BC lies inside the polygon, and point A is removed, forming triangle ABC. This process continues until the polygon is fully subdivided into triangles, and the structural surface area is the sum of these triangle areas.

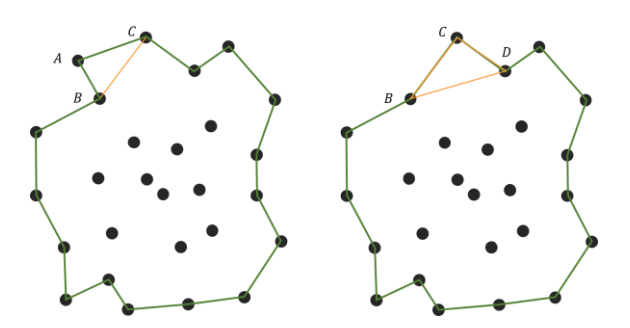


Figure 3. Extraction of the plane area using the Ear Clipping algorithm.

After obtaining the structural surface area S, an equivalent circle with the same area is used to represent the surface for simplicity and convenience in subsequent calculations. To do so, the center of the circle is defined as the mean coordinate of the surface's nodes, which serves as the centroid or the geometric center of the surface. This approach assumes that the structural surface can be approximated as a circle, simplifying the analysis. The radius is determined by the area equation $S = \pi r^2$. The radius r is then calculated to characterize the dimensional information of the structural surface.

3. Experiment

To validate the effectiveness and accuracy of the proposed method for identifying structural planes in field rock masses, a detailed experimental area was selected at an exposed rock face within a landslide located in China, as shown in Figure 4(a). The rear edge of the landslide is positioned near the top of the slope, at an elevation of approximately 3718 meters above sea level, with a vertical height difference of 834 meters from the top to the base of the slope. This significant elevation variation provides a representative section for the study of rock mass structural features. The landslide itself exhibits an elongated, planar shape, with the main sliding body presenting a wedge-like geometry, and the cross-sectional profile displaying a series of steep and gentle steps.

The landslide extends approximately 1600 meters in length, with a maximum width of around 700 meters. The primary sliding direction of the landslide ranges from 82° to 102°, indicating a clear directional movement of the mass. A total of 7,297,495 point clouds were captured from representative regions of the slope. Measurements revealed that the slope's gradient varies across its profile, with the front edge having a gradient ranging from 35° to 65°, indicating areas of moderate to steep terrain. The middle and rear sections exhibit a slightly less steep gradient, ranging from 35° to 55°. However, the back wall of the landslide features a significantly steeper local gradient, reaching up to 75°. These variations in slope gradient and topography contribute to a more complex rock mass structure, which is reflected in the point cloud data, as shown in the Figure 4(b).

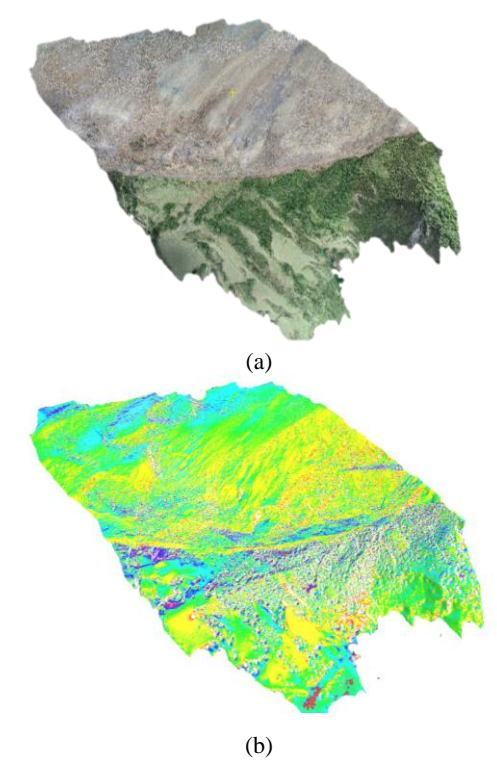


Figure 4. (a) shows the overall topographic relief of the study area of this paper. (b) illustrates the results of the point cloud preprocessing, showing the topographic details of the slope, including the slope change and related structural features. The yellow part is the steeper slope, and the green part is the relatively gentle location; the point cloud of the vegetation-covered area is not processed by the algorithm in this paper.

The algorithm presented in this paper is capable of intelligently identifying structural planes within complex rock masses. A total of 59 structural planes were successfully identified, encompassing both large, prominent planes and smaller, more intricate planes that are often challenging to detect using traditional methods. The algorithm's ability to differentiate between fine and minute planes. Each identified structural plane

is represented using distinct colors to facilitate clear differentiation and analysis. The color coding allows for easy visual identification of the various planes, providing a comprehensive overview of the spatial distribution and orientation of these features within the rock mass. As shown in Figure 5, the distinct colors correspond to individual structural planes, highlighting their respective characteristics, such as orientation, spacing, and size. This visualization aids in understanding the complexity and variability of the rock mass.

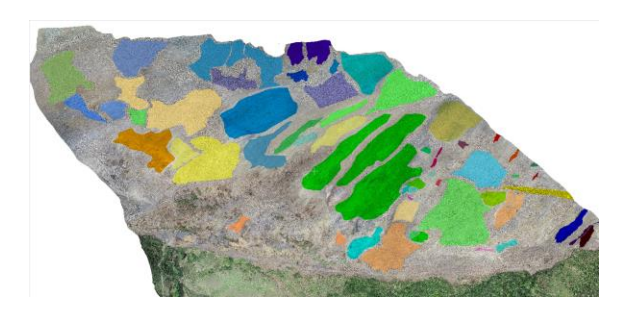


Figure 5. The rock mass structural surface extraction is realized through the algorithm in this paper.

According to the direction of the structural plane normal vector, the structural planes are divided into different dominant attitude groups, which allows a more detailed description of the rock mass. This classification result is shown in Figure 6, where each group corresponds to a set of unique structural planes with similar spatial orientation, which helps to identify key geological features and improve the accuracy of stability assessment.

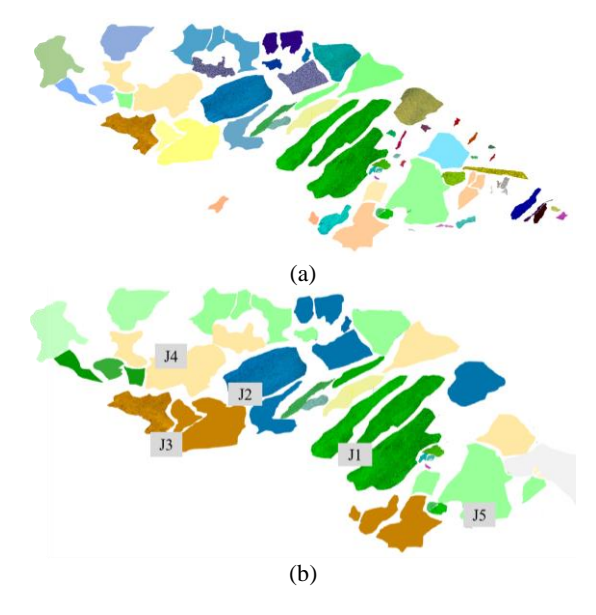


Figure 6. (a)The structural surfaces are shown without any grouping, where each individual surface is considered separately, displaying a diverse range of orientations and spatial distributions. This initial state illustrates the complexity of the rock mass, where numerous structural surfaces exist without any clear organizational structure, making it challenging to interpret the overall geological framework. (b) the structural surfaces are grouped according to the similarity in the direction of their normal vectors.

Using the extracted information regarding the structural surfaces and slope attitudes, a Zippin projection map is generated to visually represent the spatial distribution of the principal structural surface poles. As shown in Figure 7, provides an essential tool for understanding the geometric relationships between the structural surfaces, as well as their spatial orientation relative to one another. The Zippin projection method is particularly useful for visualizing pole concentrations and identifying potential weak zones or regions of instability within the slope.

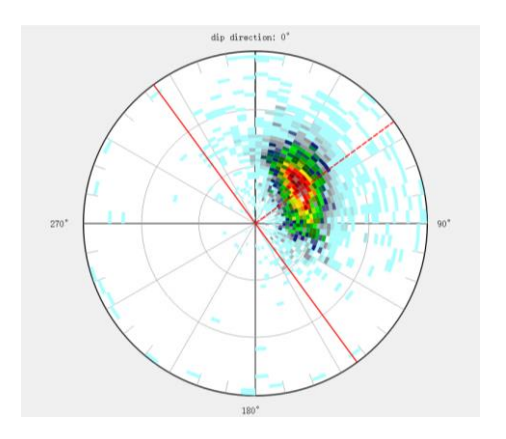


Figure 7. Stereographic projection of research area.

To quantitatively assess the accuracy and effectiveness of the proposed method, a comparison is made between the structural surface area and dimension calculations obtained using the proposed method and those calculated by CAD software, which is commonly used for precise geometric analysis. Table 1 presents a detailed comparison of the structural surface area results derived from both methods. This comparison allows for the evaluation of the proposed method's accuracy in estimating the surface areas of the structural planes, highlighting any discrepancies or alignment with the results from the CAD software. In addition to the surface area, the dimensions of the structural planes are also considered, providing further insight into the proposed method's ability to capture the true geometrical characteristics of the rock mass.

Structural		Structural	Error	Structural Surface		Error
Surface		Surface Area (m ²)	D + 0/	Dimensions (m)		D 4 0/
Group			Rate%			Rate %
	Our	CAD		Our	CAD	
J1	21.28	21.46	0.86%	3.72	3.74	0.43%
J1	15.41	15.45	0.15%	2.47	2.45	0.89%
J1	12.42	12.42	0.02%	2.18	2.18	0.32%
J1	29.55	29.53	0.05%	4.74	4.73	0.38%
J1	66.73	66.74	0.03%	7.16	7.18	0.27%
J2	17.28	17.14	0.84%	2.90	2.87	1.07%
J2	19.57	19.58	0.09%	3.27	3.29	0.34%
J2	48.56	48.61	0.12%	4.52	4.53	0.35%
J2	12.78	12.79	0.09%	2.25	2.28	0.18%
J3	41.14	40.89	0.60%	4.23	4.22	0.24%
J3	24.85	24.80	0.21%	3.81	3.80	0.26%
J3	19.21	19.17	0.21%	3.16	3.16	0.03%
J4	28.98	29.02	0.16%	4.65	4.63	0.39%
J4	13.64	13.85	1.53%	2.24	2.29	0.71%
J5	9.90	9.91	0.15%	1.69	1.70	0.59%

Table 1. Comparison of discontinuity dimension data between Polyworks and our algorithm.

From the error rates presented in Table 1, the maximum error rate for the surface area calculations does not exceed 2%, with a few instances showing an error rate as low as 1.53%. The maximum error rate for the dimension calculations does not exceed 1.07%, further validating the accuracy of the proposed method. These low error rate reflect the method's ability to correctly capture the overall size and extent of the structural planes, even in complex rock mass configurations.

The primary factor contributing to these small error rates lies in the ruggedness of the plane edges. As the structural planes often exhibit irregular and jagged edges, some edge points may be lost during the subdivision process, leading to minor inaccuracies in the final area and dimension calculations. Despite this, the overall performance of the method remains within an acceptable threshold, ensuring that it provides a reliable means for identifying and quantifying structural planes in rock masses.

4. Conclusion

This paper proposes an improved region growing algorithm based on the RANSAC algorithm and applies it to the recognition and extraction of rock mass structural surfaces from point clouds. The proposed method demonstrates excellent performance in model recognition and segmentation, particularly in regions with sharp edges, where it can effectively and comprehensively identify point cloud data. By leveraging the method presented in this study, a classification and recognition of structural surfaces in typical slope rock masses were conducted. The primary joint surfaces and bedding planes were segmented with high accuracy and completeness, allowing for the extraction of crucial information regarding the rock mass, such as the orientation, spacing, and extent of the main structural surfaces.

The effectiveness of this method is highlighted by its ability to handle complex rock mass structures, including those with intricate and irregular features. In contrast to traditional algorithms that struggle with sharp or irregular boundaries, the improved region growing algorithm maintains its robustness, ensuring the accurate identification of both fine and coarse structural features.

In addition to the structural surface segmentation, the proposed method also extracts detailed geometric information, such as the orientation and spacing of the joints, which are essential for rock mass classification, slope stability analysis, and the design of engineering structures in mountainous or geologically complex areas.

Overall, the proposed method provides a reliable and efficient tool for rock mass structural surface extraction, offering significant improvements over existing techniques. Its ability to handle complex point cloud data and accurately segment and analyze rock mass structures makes it an invaluable tool for geotechnical engineering, geological research, and other related fields.

Acknowledgements

This study was supported by National Key Research and Development Program of China, No. 2023YFB3905704.

References

- Cao, D., Ji, S., Cui, R., Liu, Q., 2022. Multi-task learning for digital rock segmentation and characteristic parameters computation. J. Pet. Sci. Eng. 208, 109202.
- Dumic, E., da Silva Cruz, L.A., 2025. Three-Dimensional Point Cloud Applications, Datasets, and Compression Methodologies for Remote Sensing: A Meta-Survey. Sensors 25, 1660.
- Gigli, G., Casagli, N., 2011. Semi-automatic extraction of rock mass structural data from high resolution LIDAR point clouds. Int. J. Rock Mech. Min. Sci. 48, 187–198.
- Haifeng, L., Lina, F., Chongcheng, C., Zhiwen, H., 2018. Roadside multiple objects extraction from mobile laser scanning point cloud based on DBN. Acta Geod. Cartogr. Sin. 47, 234.
- Liu, Y., Chen, J., Tan, C., Zhan, J., Song, S., Xu, W., Yan, J., Zhang, Y., Zhao, M., Wang, Q., 2022. Intelligent scanning for optimal rock discontinuity sets considering multiple parameters based on manifold learning combined with UAV photogrammetry. Eng. Geol. 309, 106851.
- Matsuzaki, K., Nonaka, K., 2024. Learnable Point Cloud Sampling Considering Seed Point for Neural Surface Reconstruction. IEEE Access.
- Song, S., Zhao, M., Zhang, W., Wang, F., Chen, J., Li, Y., 2024. Research on fine collection and interpretation methods of discontinuities on high-steep rock slopes based on UAV multi-angle nap-of-the-object photogrammetry. Bull. Eng. Geol. Environ. 83, 142.
- Wang, Z., Yang, L., Sheng, Y., Shen, M., 2021. Pole-like objects segmentation and multiscale classification-based fusion from mobile point clouds in road scenes. Remote Sens. 13, 4382.
- Xu, Z., Guo, G., Sun, Q., Wang, Q., Zhang, G., Ye, R., 2023. Structural plane recognition from three-dimensional laser scanning points using an improved regiongrowing algorithm based on the robust randomized Hough transform. J. Mt. Sci. 20, 3376–3391. https://doi.org/10.1007/s11629-023-7914-z